

SRINIVASAN P. MANIKANDAN  
NESAKUMAR DHARMAKKAN  
NAGAMANI SUMANA

Department of Chemical Engineering,  
Kongu Engineering College,  
Erode-638 060,  
India

SCIENTIFIC PAPER

UDC 66.021.4:62

## HEAT TRANSFER STUDIES OF $\text{Al}_2\text{O}_3$ /WATER-ETHYLENE GLYCOL NANOFUID USING FACTORIAL DESIGN ANALYSIS

### Article Highlights

- $\text{Al}_2\text{O}_3$ /ethylene glycol/water mixed nanofluid were prepared
- Natural convection heat transfer experiments were conducted based on MINITAB design matrix
- Heat transfer coefficient was analyzed by different plots as provided in MINITAB
- Model equation for calculating heat transfer coefficient was proposed based on the ANOVA results

### Abstract

*The experimental study of the heat transfer coefficient of nanofluid plays a significant role in improving the heat transfer rate of the heat exchanger. A natural convection apparatus was used to study heat transfer in the suspension of  $\text{Al}_2\text{O}_3$  nanoparticles in a water-ethylene glycol mixture base fluid. The effects of the heat input, the nanoparticle volume fraction, and the base fluid concentration on the heat transfer coefficient were studied using a  $2^3$  full factorial design matrix (16 experimental runs) and the MINITAB Design software. The levels for the heat input, nanoparticle volume fraction, and base fluid concentration were 10 and 100 W, 0.1 and 1 vol.%, and 30 and 50 vol.%, respectively. The residual, contour, 3D surface plots, and Pareto chart were drawn from the experimental results. The observed heat transfer coefficient showed the highest enhancement with the high level of the nanoparticle volume fraction and a moderate enhancement with the high level of heat input, and a slight enhancement with the base fluid concentration.*

*Keywords:*  $\text{Al}_2\text{O}_3$  nanofluid, full factorial design, heat transfer, natural convection.

“Nanofluid” attracted many researchers because of its significant application in enhancing heat transfer fluid properties such as thermal, electrical, magnetic, optical, and mechanical. Choi [1] was the first to utilize the nano-sized solid particles in conventional heat transfer fluids and showed a significant enhancement in the thermal conductivity of nanofluid. Hence the thermal performance of heat exchanger systems could be increased with the addition of nanoparticles which will save energy and the environment [2-5]. Over the years, several studies focusing on heat transfer en-

hancements using nanoparticles have been published. For instance, Das *et al.* [6] measured the thermal conductivity of  $\text{Al}_2\text{O}_3$  and CuO nanoparticle suspension in the ethylene glycol and water (EG/W) mixture using a transient hot-wire method. They observed the thermal conductivity enhancement of 20% for the 4 vol.% concentration of the prepared nanoparticles.

Wen and Ding [7] have prepared the  $\text{Al}_2\text{O}_3$  nanoparticle suspended water nanofluid and studied the heat transfer behavior of a prepared nanofluid in the laminar flow under constant wall heat flux. Their results showed that the heat transfer coefficient increases particularly at the entrance region with the increase in the Reynolds number and the nanoparticle concentration. Their result revealed that the Brownian motion of the nanoparticles resulting in the decreased thermal boundary layer is the reason for the enhancement of thermal conductivity. Cesare Biserni *et al.* [8] prepared the alumina/water nanofluid and

Correspondence: S.P. Manikandan, Department of Chemical Engineering, Kongu Engineering College, Erode-638 060, India.  
E-mail: sriperiasamy@gmail.com  
Paper received: 25 January 2021  
Paper revised: 12 May 2021  
Paper accepted: 28 May 2021

<https://doi.org/10.2298/CICEQ210125021M>

studied the natural convection of nanofluid in heterogeneous heating of square cavity. The study proposed the correlation equation to relate the Nusselt and Rayleigh numbers.

Mohebbi *et al.* [9] studied the effect of the  $\gamma$ -Al<sub>2</sub>O<sub>3</sub> nanoparticle addition in a water-based fluid on the natural convection heat transfer of the corrugated T shaped cavity. They have employed the Lattice Boltzmann method for their study. They have examined the impact of the nanoparticle Rayleigh number, solid volume fraction, and the aspect ratio of the grooves cavity on the streamlines and the averaged Nusselt number. They have obtained a positive impact on heat transfer performance by nanoparticle addition. Li and Peterson [10] studied the natural convection heat transfer of the nanofluid prepared by suspending Al<sub>2</sub>O<sub>3</sub> nanoparticles (47 nm) in water. The experiments were conducted with different particle volume fractions ranging from 0.5 to 6 vol.%. They have reported the visualization results and the causes of the deterioration of the prepared nanofluid natural convective heat transfer. Pak and Cho [11] studied the hydrodynamic effect and heat transfer behavior of the Al<sub>2</sub>O<sub>3</sub> and TiO<sub>2</sub> based nanofluid in a horizontal circular tube. They found that the Nusselt number for the fully developed turbulent flow enhanced significantly concerning the nanoparticle volume fraction and the Reynolds number. They have proposed a new correlation for the turbulent convective heat transfer in nanofluids. Maiga *et al.* [12] used the Al<sub>2</sub>O<sub>3</sub>/ethylene glycol, and Al<sub>2</sub>O<sub>3</sub>/water nanofluids were to investigate the turbulent and laminar flow effect of a nanofluid inside circular tubes. They found that the heat transfer enhancement was higher for the Al<sub>2</sub>O<sub>3</sub>/ethylene glycol nanofluid when compared to the Al<sub>2</sub>O<sub>3</sub>/water nanofluid. The experimental study performed for the Al<sub>2</sub>O<sub>3</sub>-water mixture by Nguyen *et al.* [13] showed the enhancement in the heat transfer coefficient by 40% at 6.8 vol.% of nanoparticles. Al<sub>2</sub>O<sub>3</sub>/water nanofluid was used by Pandey *et al.* [14] to investigate the heat transfer performance of the prepared nanofluid in a counter flow corrugated plate heat exchanger. They studied the impact of nanofluid and water as coolants on heat transfer, frictional losses, and exergy loss. It was noted that the heat transfer behavior improves with the decrease in the nanoparticle concentration for water-nanofluid systems.

Prasad *et al.* [15] studied the heat transfer effect and friction of Al<sub>2</sub>O<sub>3</sub> nanoparticles dispersed in water in a U-tube heat exchanger. They determined the Nusselt number at various Reynolds numbers and different nanoparticle volume fractions. The study concludes that the maximum increment in the Nusselt number occurs with the maximum Reynolds number.

Huang *et al.* [16] used Al<sub>2</sub>O<sub>3</sub> to study the effect of the Al<sub>2</sub>O<sub>3</sub>/water nanofluid on heat transfer and pressure drop characteristics in a chevron-type plate heat exchanger. The study showed that at a constant Reynolds number, the heat transfer enhancement in the nanofluid was better than that in the base fluid. The heat transfer enhancement may be due to the increase in thermal conductivity. Xie *et al.* [17] prepared a nanofluid with different metal oxide suspensions of nanoparticles (Al<sub>2</sub>O<sub>3</sub>, ZnO, SiO<sub>2</sub>, MgO, and TiO<sub>2</sub>) in ethylene glycol. The study focused on the thermal conductivity and heat transfer effects. According to their research, the MgO/EG nanofluid showed the highest heat transfer enhancement with 41% improvement in thermal conductivity compared with other suspensions at a volume concentration of 5%.

Satti *et al.* [18] studied thermal conductivity in the ZnO, Al<sub>2</sub>O<sub>3</sub>, CuO, and SiO<sub>2</sub> nanoparticle suspensions in a water and propylene glycol mixture base fluid. Their operating conditions were temperature ranging from 30 to 90°C and a nanoparticle concentration up to 6 vol.%. Their findings were the thermal conductivity proportionately increases with the nanoparticle concentration and the operating temperature. This result shows that the nanofluid could be utilized for higher temperature applications. Thermal conductivity and heat transfer behavior of graphene, TiO<sub>2</sub>, and ZnO nanoparticles suspended in an ethylene glycol-water mixture was analyzed by Periasamy and Baskar [19-21]. Their analysis revealed that the thermal conductivity and the heat transfer coefficient were enhanced by increasing the nanoparticle volume fraction. Sahoo *et al.* [22] and Yu *et al.* [23] observed that as the nanoparticle loading of Al<sub>2</sub>O<sub>3</sub> in the 40:60 (water: ethylene glycol) mixture by mass ratio increased, the viscosity of the nanofluid also increased. Huang *et al.* [24] studied the heat transfer characteristics experimentally using Al<sub>2</sub>O<sub>3</sub> nanoparticles in a plate heat exchanger. They concluded that the heat transfer enhanced significantly at a constant Reynolds number than the base fluid without nanoparticles. The thermal conductivity enhancement is the reason for this heat transfer enhancement.

Based on the literature survey, several studies were found concerning the application of nanofluids in heat transfer for improving the efficiency of a heat exchanger. However, the full factorial design has rarely been used to analyze the influence of various input factors on the heat transfer characteristics of nanofluids. In this study, a natural convection heat transfer apparatus was used, whereas Al<sub>2</sub>O<sub>3</sub> nanoparticles were suspended in a base fluid mixture of water-ethylene glycol. The effects of input factors such as the heat input, the nanoparticle volume fraction

and the base fluid concentration on the experimental heat transfer coefficient ( $h_{exp,nf}$ ) were analyzed using the residual plot, Pareto chart, contour plot, and 3D surface plot.

## MATERIALS AND METHODS

### Experimental procedure

The experiment was conducted in a natural convection experimental setup. The schematic layout and photography of the experimental setup are shown in Figure 1. The experimental setup consists of a vertical stainless steel (SS) tube enclosed in a duct. The diameter and length of the tube are 0.045 m and 0.5 m, respectively. The front side of the rectangular duct is made of a transparent section to facilitate visual observation. The heating was conducted by an electrical heating element embedded in a copper tube. The thermocouples were inserted along the tube to measure the surface temperature at various heights. The tube surface was polished to minimize radiation loss. An ammeter and voltmeter were used for determining the wattage dissipated by the heat source.

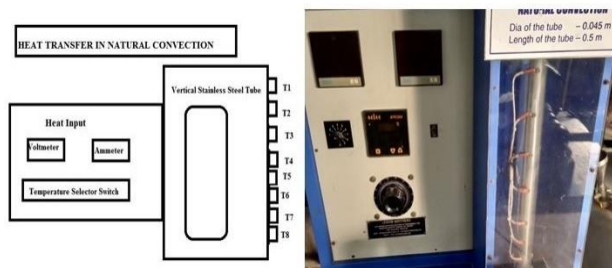


Figure 1. Schematic layout and photography of the experimental set up.

The input factors were employed in the experiment as per the design matrix. After the steady-state attainment, the temperatures  $T_1$  to  $T_8$  were noted down. In addition, the ambient temperature was recorded. The experiment was repeated for different input factors based on the MINITAB DOE results. The convective heat transfer coefficient was calculated by the following formulae.

$$h_{exp,nf} = \frac{Q}{A(T_s - T_a)}$$

where  $T_s$  is the surface temperature calculated as the average temperature between  $T_2$  and  $T_7$ ,  $T_a$  is ambient temperature calculated as the average temperature between  $T_1$  and  $T_8$ , and  $A$  is the tube surface.

### Factorial design and analysis

#### Input parameters and their levels

The experiments were conducted at all combinations of the factor levels, as provided by the

design software, and the output response (heat transfer coefficient) was determined. Each experimental operating condition was a "Run", the output response was an "Observation," and the entire set of runs was the "Design." [25-27]. A two-level full factorial design was employed with two replications, which provides 16 experimental combinations. Table 1 provides the design summary and factor and level for the full factorial design applied in the present study.

Table 1. Design summary: factor and level for the full factorial design

Factors	Level		
Base design			
Number of experimental runs			
Replicates			
Blocks			
Input Factors	Code	Low	High
Heat Input, W	A	10	100
Nanoparticle volume fraction, vol. %	B	0.1	1.0
Base fluid volume fraction, vol. %	C	30	50

Statistical analysis was applied to investigate the significance of the input factors and their interactions on the output response. Table 2 exhibits the experimental results of the  $2^3$  full factorial design.

#### Stepwise regression model for elimination of insignificant factors

The stepwise regression method was used in MINITAB to eliminate the nonsignificant factors. Minitab added or removed a term in the stepwise analysis in each step. In addition, a mixed selection approach, i.e., a combination of the forward and backward selection of variables, is used. The results of the stepwise regression model were tabulated and shown in Table 3. Since the values of  $R^2$  and  $R^2_{adj}$  were close to each other, the model did not include insignificant parameters [28]. The developed regression equation in its coded form is provided below.

$$h_{nf} = 0.258A + 43.6B + 1.24C - 15.2$$

## RESULTS AND DISCUSSION

### Residual plots for the heat transfer coefficient of Al<sub>2</sub>O<sub>3</sub>/EG/W nanofluids

In statistics, a residual plot is used for finding the fitness of data for the performed experimental results. A residual plot is drawn by taking the independent variable on the horizontal axis and the residual values on the vertical. Figure 2 presents the residuals versus

Table 2. Experimental results of 2<sup>3</sup> full factorial design

Standard order	Run order	Factorial input variable			Response variable, $h_{exp,nf}$ , (W/m <sup>2</sup> K)
		A Heat Input, Q (W)	B Nanoparticle volume fraction (vol.%)	C Base fluid volume fraction (vol.%)	
1	4	100	1.0	50	114
2	1	10	0.1	30	28
3	3	10	1.0	50	102
4	5	10	0.1	30	31
5	7	10	1.0	50	92
6	6	100	0.1	30	42
7	8	100	1.0	50	108
8	2	100	0.1	30	48
9	15	10	1.0	50	87
10	14	100	0.1	30	65
11	12	100	1.0	50	118
12	9	10	0.1	30	30
13	11	10	1.0	50	82
14	10	100	0.1	30	38
15	16	100	1.0	50	106
16	13	10	0.1	30	33

Table 3. Factorial fit and stepwise regression results for  $h$ ,  $nf$  versus A, B, C

Term	Coef	SE Coef	T	P
Constant	-15.13	11.28	-1.35	0.203
A	0.25833	0.05609	4.61	0.001
B	43.611	5.609	7.78	0.000
C	1.2375	0.2524	4.90	0.000
S	10.096			
R-Sq	89.8%			
R-Sq(adj)	87.3%			

Source	DF	Seq SS	MS	F	P
Regression	3	10774.7	3591.6	35.23	0.000
Residual error	12	1223.3		101.9	
Pure error	8	31.5			
Total	15	11998			

the fitted values, histogram, and the residuals versus the order of the data for the convective heat transfer coefficient. Based on the present study, most of the data are linearly associated, and hence the model is best fitted with the obtained data. The residual plot also shows the interaction between the input factors and the output response. All these residual plots clearly show the fitness of the present research data. A good fit within the limit is also observed, indicating no unexpected errors in the developed model [29].

#### Pareto chart for the heat transfer coefficient of Al<sub>2</sub>O<sub>3</sub>/EG/W nanofluids

Pareto chart is very useful in identifying the significant factors and their interactions on the response factor for the given experimental results [30].

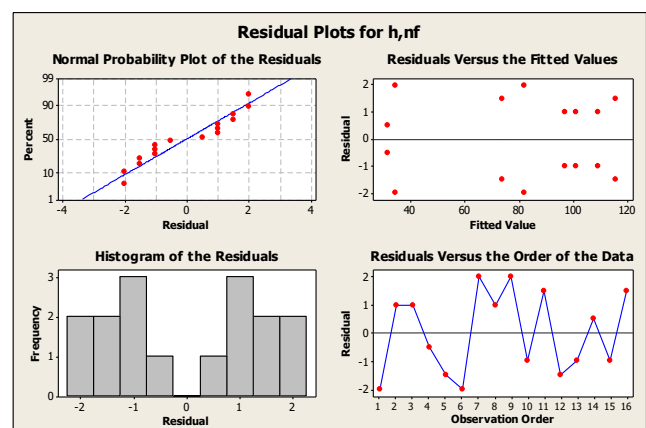


Figure 2. Residual plots for heat transfer coefficient of nanofluids.

The Pareto chart is plotted with the response factor of the convective heat transfer coefficient to segregate the crucial factors from insignificant factors. Figure 3 shows the Pareto chart of the standardized effects on the heat transfer coefficient of nanofluids. In this Figure, the bars represent factors *B* (nanoparticle volume fraction), *A* (heat input), *AB* (interaction of *A* and *B*), and *C* (base fluid volume fraction) cross the reference line (i.e., 2.31). These factors are statistically significant at the 0.05 level with the current model terms.

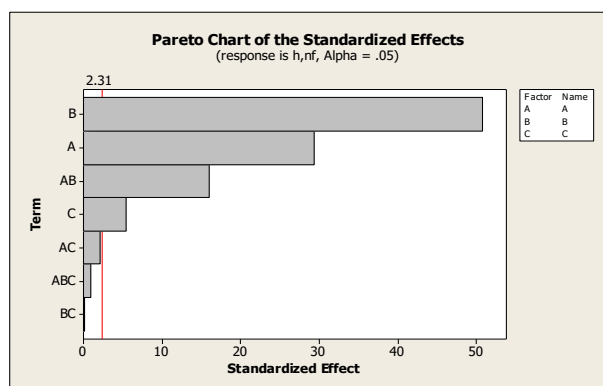


Figure 3. Pareto chart of the standardized effects on heat transfer coefficient of Nanofluids.

### Contour plot for heat transfer coefficient of Al<sub>2</sub>O<sub>3</sub>/EG/W nanofluids

The effects of the process variables, such as the heat input, nanoparticle volume fraction, and base fluid concentration, are optimized by the full factorial design. A three-dimensional contour plot was drawn from the developed model, as shown in Figures 4(a) and (b). Figure 4(a) depicts the contour plot for the heat transfer coefficient concerning the input factors *A* and *C*. A contour plot shows a 2-dimensional view in which all points with the same response are linked to produce contour lines. Contour plots help investigate the effect on the desired response for the operating conditions. It was observed from figure 4(a) that the heat transfer coefficient (output response) varies between the ranges from 45 W/(m<sup>2</sup>K) to 105 W/(m<sup>2</sup>K) based on the variations on both *A* (heat input) and *C* (base fluid volume fraction). With increasing the heat input and the base fluid concentration, the heat transfer coefficient increases significantly, which shows that the heat input and the base fluid concentration favor the heat transfer enhancement.

Figure 4(b) provides the contour plot for the heat transfer coefficient for the input factors *A* and *B*. The heat transfer coefficient increases gradually for the heat input and the nanoparticle volume fraction. The maximum enhancement of 105 W/(m<sup>2</sup>K) was

observed at the heat input of 100 W and the nanoparticle volume fraction of 1.0 vol.%. This result shows that the nanoparticle addition significantly enhances the heat transfer characteristics of the base fluid used in industries.

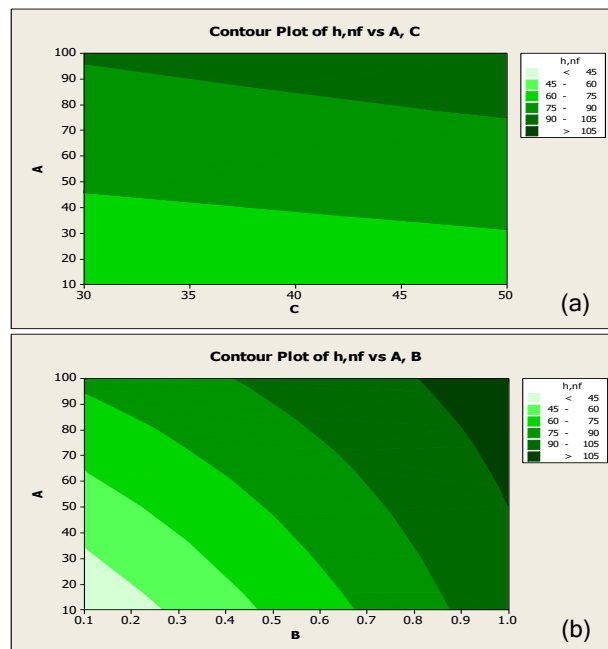


Figure 4. Contour plot for heat transfer coefficient of nanofluids.

### 3D surface plot for the heat transfer coefficient of Al<sub>2</sub>O<sub>3</sub>/EG/W nanofluids

The surface plot for the heat transfer coefficient concerning input factors *B* and *A* is shown in Figure 5. The heat transfer coefficient increases gradually for the nanoparticle volume fraction and the heat input. The maximum thermal conductivity enhancement was observed at a nanoparticle fraction of 1.0 vol.% and heat input of 100 W.

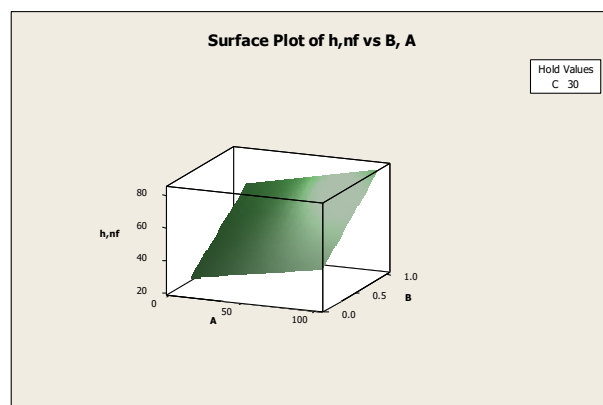


Figure 5. 3D surface plot for heat transfer coefficient of nanofluids.

An experiment was performed at the optimum conditions to validate the developed equation. As a result, a good agreement between the experimental

values and the values calculated by the developed equation was observed. Furthermore, it was also noticed that the heat transfer coefficient variations fall within  $\pm 5\%$  deviation, which shows the accuracy of the developed equation.

## CONCLUSION

The effect on the heat transfer coefficient of the Al<sub>2</sub>O<sub>3</sub> nanoparticle suspended ethylene glycol/water base fluid was analyzed using the 2<sup>3</sup> full factorial design matrix and the MINITAB design software. The influence of the heat input (*A*), nanoparticle volume fraction (*B*), and base fluid volume fraction (*C*) was studied in a natural convection heat transfer apparatus. The obtained results were analyzed by plotting residual, contour, 3D surface plots, and the Pareto chart. Based on the residual plot, most of the data are linearly fitted, and hence the model is best fitted for the present study. The maximum heat transfer coefficient of 125 W/(m<sup>2</sup>K) was observed corresponding to the heat input of 100 W, the nanoparticle fraction of 1.0 vol.%, and the 50 vol.% base fluid concentration. It may be concluded from the results of the contour and surface plots that the heat transfer coefficient increases gradually by increasing the heat input, nanoparticle concentration, and base fluid concentration.

## Acknowledgment

The authors thank the management of Kongu Engineering College for the contribution of the SEED Grand and the Department of Chemical Engineering for the facility provided.

## REFERENCES

- [1] S.U.S. Choi, S. Lee, S. Li, J.A. Eastman, *J. Heat Transfer* 121 (1999) 280-289.
- [2] I.M. Shahrul, I.M. Mahbubul, R. Saidur, S.S. Khaleduzzaman, M.F.M. Sabri, M.M. Rahman, *Numer. Heat Transfer Part A: Appl.* 65 (2014) 699-713.
- [3] I.M. Shahrul, I.M. Mahbubul, R. Saidur, M.F.M. Sabri, S.S. Khaleduzzaman, *J. Chem. Eng. Jpn.* 47 (2014) 340-344.
- [4] I.M. Shahrul, I.M. Mahbubul, R. Saidur, M.F.M. Sabri, M.A. Amalina, S.S. Khaleduzzaman, *Adv. Mater. Res.* 832 (2014) 154-159.
- [5] C.Y. Lin, J.C. Wang, T.C. Chen, *Appl. Energy* 88 (2011) 4527-4533.
- [6] S.K. Das, N. Putra, P. Thiesen, W. Roetzel, *J. Heat Transfer* 125 (2003) 567-574.
- [7] D. Wen, Y. Ding, *Int. J. Heat Mass Transfer* 47 (2004) 5181-5188.
- [8] I. Rashidi, O. Mahian, G. Lorenzini, C. Biserni, S. Wongwises, *Int. J. Heat Mass Transfer* 74 (2014) 391-402.
- [9] R. Mohebbi, S. H. Khalilabad, Y. Ma, *J. Appl. Fluid Mech.* 12 (2019) 1151-1160.
- [10] H.C. Li, G.P. Peterson, *Adv. Mech. Eng.* 2 (2010) 1-10.
- [11] B.C. Pak, Y. Cho, *Exp. Heat Transfer* 11 (1998) 151-170.
- [12] S.E.B. Maiga, C.T. Nguyen, N. Galanis, G. Roy, *Superlattices Microstruct.* 35 (2004) 543-557.
- [13] C.T. Nguyen, G. Roy, C. Gauthier, N. Galanis, *Appl. Therm. Eng.* 27 (2007) 1501-1506.
- [14] S.D. Pandey, V.K. Nema, *Exp. Therm. Fluid Sci.* 38 (2012) 248-256.
- [15] P.V. Durga Prasad, S. Gupta, M. Sreeramulu, L.S. Sundar, M.K. Singh, A.C.M. Sousa, *Exp. Therm. Fluid Sci.* 62 (2015) 141-150.
- [16] D. Huang, Z. Wu, B. Sunden, *Int. J. Heat Mass Transfer* 89 (2015) 620-626.
- [17] H. Xie, W. Yu, W. Chen, *J. Exp. Nanosci.* 5 (2010) 463-472.
- [18] J.R. Satti, D.K. Das, D. Ray, *Int. J. Heat Mass Transfer* 107 (2017) 871-881.
- [19] S.P. Manikandan, R. Baskar, *Chem. Ind. Chem. Eng. Q.* 24 (2018) 309-318.
- [20] S.P. Manikandan, R. Baskar, *Chem. Ind. Chem. Eng. Q.* 27 (2021) 15-20.
- [21] S.P. Manikandan, R. Baskar, *Chem. Ind. Chem. Eng. Q.* 27 (2021) 177-187.
- [22] B.C. Sahoo, R.S. Vajjha, R. Ganguli, G.A. Chukwu, D.K. Das, *Pet. Sci. Technol.* 27 (2009) 1757-1770.
- [23] W. Yu, H. Xie, Y. Li, L. Chen, Q. Wang, *Powder Technol.* 230 (2012) 14-19.
- [24] D. Huang, Z. Wu, B. Sunden, *Exp. Therm. Fluid Sci.* 72 (2016) 190-196.
- [25] R. V. Lenth, *Technometrics* 31 (1989) 469-473.
- [26] R. L. Plackett, J. P. Burman, *Biometrika* 33 (1946) 305-325.
- [27] H. Rostamian, M. N. Lotfollahi, *Period. Polytech. Chem. Eng.* 60 (2016) 93-97.
- [28] B.L. Dehkordi, A. Ghadimi, S.C. Henk, *Metselaar, J. Nanopart. Res.* 15 (2013) 1-9.
- [29] S.P. Manikandan, R. Baskar, *Period. Polytech. Chem. Eng.* 62 (2018) 317-322.
- [30] M. Khajeh, *Food Chem.* 129 (2011) 1832- 1838.

SRINIVASAN P. MANIKANDAN  
NESAKUMAR DHARMAKKAN  
NAGAMANI SUMANA

Department of Chemical Engineering,  
Kongu Engineering College,  
Erode-638 060,  
India

NAUČNI RAD

## ISTRAŽIVANJE PRENOSA TOPLOTE U NANOFLUIDU $Al_2O_3$ /VODA-ETILEN GLIKOL KORIŠĆENJEM FAKTORIJALNOG DIZAJNA

*Eksperimentalno proučavanje koeficijenta prenosa toplote u nanofluidima igra značajnu ulogu u poboljšanju brzine prenosa toplote izmenjivača toplote. Aparatura za prirodnu konvekciju je korišćena za proučavanje prenosa toplote u suspenziji nanočestica  $Al_2O_3$  u mešavini voda-etilen glikol kao osnovnog fluida. Efekti unosa toplote, zapreminskog udela nanočestica i koncentracije osnovnog fluida na koeficijent prenosa toplote proučavani su korišćenjem  $2^3$  punog faktorijalnog plana (16 eksperimenata) i softvera MINITAB Design. Nivoi za unos toplote, zapreminski udeo nanočestica i koncentracija osnovnog fluida bili su 10 W i 100 W, 0,1% i 1% v/v i 30% and 50% v/v, redom. Na osnovu eksperimentalnih podataka, nacrtani su rezidualni, konturni i 3D površinski grafici, kao i Pareto grafikon. Najveće poboljšanje koeficijenta prenosa toplote postignuto je pri visokom nivou zapreminskog udela nanočestica, umereno poboljšanje sa visokim nivoom toplotnog unosa, a blago poboljšanje sa koncentracijom baznog fluida.*

*Ključne reči:  $Al_2O_3$  nanofluid, puni faktorijalni plan, prenos toplote, prirodna konvekcija.*

